

# Calculation of Partition Coefficient of an Unstable Compound Using Kinetic Methods

PETER R. BYRON\*, ROBERT E. NOTARI<sup>‡</sup>, and ERIC TOMLINSON

Received June 27, 1979, from the College of Pharmacy, Ohio State University, Columbus, OH 43210. Accepted for publication December 6, 1979. \*Present address: Department of Pharmacy, University of Aston in Birmingham, Birmingham, B4 7ET, England.

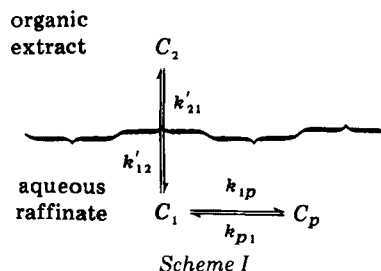
**Abstract** □ A stirred transfer cell containing equal volumes of light liquid paraffin and an aqueous phase at 37° was used to demonstrate the feasibility of calculating the partition coefficient of an unstable compound by kinetic analysis. Cyclohept-2-enone was chosen since it is a neutral molecule and, therefore, should have a pH-independent oil-water partition coefficient,  $K_D$ . Moreover, this cyclic  $\alpha,\beta$ -unsaturated ketone undergoes hydrogen-ion-catalyzed hydration but is sufficiently stable at neutral pH to determine  $K_D$ . The model system chosen represents first-order transfer between the aqueous ( $C_1$ ) and organic ( $C_2$ ) phases with simultaneous, reversible, first-order hydration. The transfer constants,  $k'_{12}$  and  $k'_{21}$ , were determined at 37° in the absence of degradation where asymptotic values for  $C_1$  agreed with the observed equilibrium values in nonkinetic partitioning studies. The first-order rate constants for hydration in 0.1 N HCl were determined at 37° in the absence of the organic phase. Partitioning with simultaneous hydration then was studied using 0.1 N HCl and light liquid paraffin. Data were analyzed by nonlinear regression based on the equation for  $C_1$  as a function of time. The values for  $k'_{12}$  and  $k'_{21}$  from these experiments were comparable to the estimates obtained under stable conditions. This agreement demonstrates that simultaneous degradation and partitioning can be analyzed for  $k'_{12}$  and  $k'_{21}$ , thus permitting calculation of the partition coefficient (*i.e.*,  $K_D = k'_{12}/k'_{21}$ ) that would be observed if the drug were stable.

**Keyphrases** □ Partition coefficients—unstable compounds, cyclohept-2-enone, calculation by kinetic methods □ Cyclohept-2-enone—partition coefficient, calculation by kinetic methods □ Drug partitioning—unstable compounds, cyclohept-2-enone, calculation of partition coefficient by kinetic methods

The two-film theory proposed by Lewis and Whitman (1, 2) for the kinetics of solute transfer between two liquid phases was first experimentally verified by Gordon and Sherwood (3, 4) using a stirred transfer cell (Fig. 1). Since then, both the cell and the theory have been studied extensively and discussed (5–7). A transfer cell was employed to measure the rates of helium and isobutane mass transfer from water to toluene and decahydronaphthalene (8). The diffusion of salts across a butanol–water interface was studied at 13–40°, and the Arrhenius parameters were compared with those for uptake of ions by frog muscle (9). An interesting application of this cell to a drug involved a study that demonstrated ion-pair formation in the transfer of dextromethorphanium ions from water to chloroform (10). McNulty (11) employed a stirred transfer cell to study the effect of polysorbate 60 on the cholesterol uptake by vegetable oil from an aqueous solution containing 5% isopropanol.

The three-phase transfer cell of Rosano *et al.* (12) frequently has been applied to pharmaceutical problems. Lippold and Schneider (13–16) determined the forward ( $k_f$ ; aqueous to organic) and reverse ( $k_r$ ) rate constants for a homologous series of benzoic acid quaternary esters. Kubinyi (17) used these data to show that  $\log k_f$  and  $\log k_r$  can be defined as a function of the number ( $n$ ) of  $\text{CH}_2$  groups in a homologous series, provided that  $\log K_D$  also is a simple function of  $n$ , where  $K_D$  is the partition coefficient.

This report demonstrates that the partition coefficient



may be calculated from data representing the partitioning kinetics in a simple transfer cell (Fig. 1) when a drug undergoes simultaneous degradation in the aqueous phase. The two-phase cell was chosen to accommodate the added complexity introduced by drug instability in the aqueous phase. The model system (cyclohept-2-enone partitioning between liquid petrolatum and water or aqueous hydrochloric acid) chosen to test this theory allows independent evaluation of each rate constant in Scheme I, which represents partitioning in a stirred transfer cell with a competing reversible reaction in the aqueous phase. The concentration of cyclohept-2-enone in the extract (liquid petrolatum) is represented by  $C_2$ , and that in the raffinate (aqueous phase) is represented by  $C_1$ . The concentration of the degradation product,  $C_p$ , is limited to the aqueous phase, which is consistent with the experimental results. Rate constants are apparent first order, and the initial conditions are  $C_1 = C_1^0$  with  $C_2 = C_p = 0$ .

## THEORY

**Partitioning Kinetics with Stable Drug**—For the case where the partition coefficient,  $K_D$ , remains constant over the concentration range of the transfer experiment, the observed value may be defined by:

$$K_D = C_2^*/C_1^* \quad (\text{Eq. 1})$$

where  $C_2^*$  and  $C_1^*$  are the equilibrium concentrations in the raffinate ( $C_1$ ) and the organic extract ( $C_2$ ). At any time during a kinetic run (according to the two-film theory):

$$K_D = C_2^*/C_1^* = C_{2i}/C_{1i} = C_2/C_1 \quad (\text{Eq. 2})$$

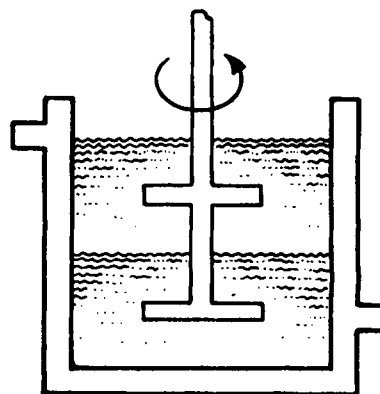
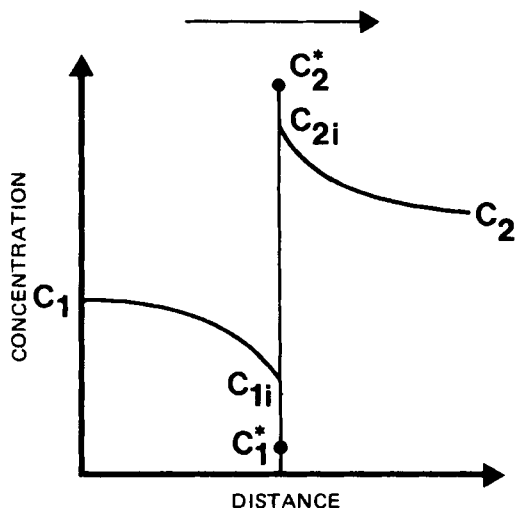


Figure 1—Schematic diagram of a two-phase transfer cell with a jacketed beaker for constant-temperature control.



**Figure 2**—Concentration gradients in a two-phase transfer cell. The arrow at the top indicates the direction of mass transfer. The concentration of diffusing solute in various regions is defined as: the average or mixed concentration in the stirred raffinate ( $C_1$ ) and extract ( $C_2$ ); at the interface on the raffinate side ( $C_{1i}$ ) and extract side ( $C_{2i}$ );  $C_1^* = C_2/K_D$ ; and  $C_2^* = C_1/K_D$ .

The symbols are defined in Fig. 2. The solute transfer rate from the bulk of the raffinate to the interface through the diffusion layer is dependent on Fick's first law and may be written as:

$$J = -da/dt = V_1(-dC_1/dt) = (C_1 - C_{1i})(D_1A/h_1) \quad (\text{Eq. 3})$$

where  $a$  is the amount of solute in the raffinate,  $V_1$  is the volume of the raffinate,  $A$  is the interfacial area, and  $D_1$  and  $h_1$  are the diffusion coefficient and thickness of the diffusion layer in the raffinate, respectively. Similarly, the transfer rate from the interface to the bulk of the extract may be written as:

$$J = (C_{2i} - C_2)(D_2A/h_2) \quad (\text{Eq. 4})$$

Provided that the interfacial barrier has no significant resistance and that thermal, electrical, and osmotic gradients are absent, then application of the two-film theory enables the overall transfer rate to be defined in terms of the overall concentration gradient  $[C_1 - (C_2/K_D)]$  as:

$$J = k_{12}A(C_1 - C_1^*) \quad (\text{Eq. 5})$$

since  $C_1^*$  is defined as  $(C_2/K_D)$  in Eq. 2. According to Flynn *et al.* (18), the overall rate constant for transfer from the raffinate to the extract,  $k_{12}$ , can be calculated from:

$$R_T = \frac{1}{k_{12}} = \frac{h_1}{D_1} + \frac{h_2}{D_2K_D} \quad (\text{Eq. 6})$$

where  $R_T$  (the diffusional resistance) is the sum of the individual resistances. Equation 6 assumes the validity of the two-film theory and allows the derivation of Eq. 5 from Eqs. 2-4. Equation 5 is the form of the rate expression generally found in the literature (1-7). Its use requires analysis of both the raffinate and extract to determine  $C_1 - C_1^*$  experimentally.

Since  $C_1^* = C_2/K_D$  and the amount of solute in the extract,  $b$ , may be calculated from  $b = a_0 - a$ , Eq. 5 also may be written as:

$$J = \frac{-da}{dt} = k_{12}A \left[ \left( \frac{a}{V_1} \right) - \left( \frac{a_0 - a}{K_D V_2} \right) \right] \quad (\text{Eq. 7})$$

where  $V_2$  is the volume of the extract, and the amount of solute in the interface is negligible. Integration of Eq. 7 from  $t = 0$  to  $t$  and from  $a = a_0$  to  $a$ , followed by substitution of  $a_\infty$  for  $[a_0 V_1 / (K_D V_2 + V_1)]$ , yields:

$$\ln(a - a_\infty) = \ln(a_0 - a_\infty) - St \quad (\text{Eq. 8})$$

which also may be written as:

$$(a - a_\infty) = (a_0 - a_\infty)e^{-St} \quad (\text{Eq. 9})$$

Dividing by  $V_1$  allows conversion of Eq. 9 to concentration:

$$(C_1 - C_1^*) = (C_1^0 - C_1^*)e^{-St} \quad (\text{Eq. 10})$$

Thus, a plot of  $\ln(a - a_\infty)$  or  $\ln(C_1 - C_1^*)$  versus time is linear with a negative slope,  $S$ , defined by:

$$S = \left[ \frac{A(K_D V_2 + V_1)}{K_D V_1 V_2} \right] k_{12} \quad (\text{Eq. 11})$$

which may be used to calculate the overall rate constant for transfer from the raffinate to the extract. The  $S$  value is equivalent to the stirred cell transfer rate constant,  $S_{SC}$ , calculated by McNulty (11).

Solving for  $k_{12}$  in Eq. 6 and substituting in Eq. 11 yield:

$$S = \frac{D_1 D_2 A (K_D V_2 + V_1)}{V_1 V_2 (D_2 K_D h_1 + D_1 h_2)} \quad (\text{Eq. 12})$$

In a transfer cell, the interfacial area, phase volumes, and stirring rate may be kept constant throughout the experiment. In these studies,  $V_1 = V_2 = V$ , while  $D_1$ ,  $D_2$ ,  $h_1$ ,  $h_2$ , and  $A$  remain constant, which leads to:

$$S = \left[ \frac{A(K_D + 1)}{V K_D} \right] k_{12} = \frac{k'_{12}(K_D + 1)}{K_D} \quad (\text{Eq. 13})$$

where  $k'_{12}$  is expressed in reciprocal time and is the apparent first-order forward rate constant for the partitioning process (Scheme I). Thus:

$$k'_{12} = D_1 D_2 A K_D / V (D_2 K_D h_1 + D_1 h_2) = k_{12} A / V \quad (\text{Eq. 14})$$

For data representing the extract, an equation similar to Eq. 5 may be written:

$$J = k_{21}A(C_2^* - C_2) \quad (\text{Eq. 15})$$

Since  $C_2^* = C_1/K_D$  and  $a = a_0 - b$ , Eq. 15 may be rewritten as:

$$\frac{db}{dt} = k_{21}A \left[ \frac{(a_0 - b)K_D}{V_1} - \left( \frac{b}{V_2} \right) \right] \quad (\text{Eq. 16})$$

which, after integrating between the limits  $t = 0$  to  $t$  and  $b = 0$  to  $b$  and substituting  $b_\infty$  for  $[a_0 K_D V_2 / (K_D V_2 + V_1)]$ , yields:

$$\ln(b_\infty - b) = \ln b_\infty - S't \quad (\text{Eq. 17})$$

Division of the exponential form of Eq. 17 by  $V_2$  allows conversion to  $C_2$ . A plot of  $\ln(b_\infty - b)$  or  $\ln(C_2^* - C_2)$  versus time is linear with a negative slope,  $S'$ , defined by:

$$S' = \left[ \frac{A(K_D V_2 + V_1)}{V_1 V_2} \right] k_{21} \quad (\text{Eq. 18})$$

With the assumption that  $V_1 = V_2 = V$ , Eq. 18 reduces to:

$$S' = \left[ \frac{A(K_D + 1)}{V} \right] k_{21} \quad (\text{Eq. 19})$$

and the apparent first-order reverse rate constant for the partitioning process (Scheme I) is:

$$k'_{21} = \frac{S'}{(K_D + 1)} \quad (\text{Eq. 20})$$

where  $k'_{21} = k_{21}A/V$ . Since mass balance requires that:

$$\frac{-da}{dt} = \frac{db}{dt} \quad (\text{Eq. 21})$$

then  $S = S'$ , and the observed slopes of first-order plots based on Eqs. 8 and 17 are equal. Therefore, Eq. 13 equals Eq. 19 and:

$$S = S' = \left[ \frac{A(K_D + 1)}{V K_D} \right] k_{12} = \left[ \frac{A(K_D + 1)}{V} \right] k_{21} \quad (\text{Eq. 22})$$

Therefore:

$$K_D = (k_{12}/k_{21}) = (k'_{12}/k'_{21}) \quad (\text{Eq. 23})$$

Thus, the partition coefficient,  $K_D$ , is the ratio of the forward and reverse rate constants.

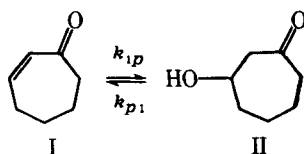
From Eqs. 13 and 20, it can be shown that:

$$(k'_{12} + k'_{21}) = S = S' \quad (\text{Eq. 24})$$

Thus, the negative slope of a first-order plot for concentration in the raffinate (Eq. 10) or the extract (Eq. 17) equals the observed first-order rate constant,  $k_{obs}$ , which is the sum of the constants,  $k'_{12} + k'_{21}$ , whose ratio ( $k'_{12}/k'_{21}$ ) is the partition coefficient,  $K_D$ .

**Simultaneous Partitioning and Reversible Aqueous Degradation**—Scheme I represents simultaneous first-order partitioning with reversible aqueous degradation to a nonpartitioning product. Solving (19) the corresponding equation for  $-dC_1/dt$  and setting  $A$  constant and  $V_1 = V_2$  yields:

$$C_1 = X e^{-\gamma t} + Y e^{-\delta t} + Z \quad (\text{Eq. 25})$$



Scheme II

where  $X = C_1^0(k'_{21} - \gamma)(k_{p1} - \gamma)/\gamma(\gamma - \delta)$ ,  $Y = C_1^0(k'_{21} - \delta)(k_{p1} - \delta)/\delta(\delta - \gamma)$ ,  $Z = C_1^0 k_{21} k_{p1} / \gamma \delta$ ,  $\gamma = 0.5(K_1 + \sqrt{K_1^2 - 4K_2})$ ,  $\delta = 0.5(K_1 - \sqrt{K_1^2 - 4K_2})$ ,  $K_1 = (k'_{12} + k'_{21} + k_{1p} + k_{p1})$ , and  $K_2 = (k'_{12} k_{p1} + k'_{21} k_{p1} + k_{21} k_{1p})$ . If partitioning of the product into the organic extract is significant, then Scheme I and Eq. 25 must be modified to include the additional compartment,  $C_{2p}$ . The aqueous degradation of drugs usually goes to completion (i.e., apparent irreversibility), and the time course for  $C_1$  therefore is independent of  $C_p$ . This case, in which the partitioning behavior of the product is immaterial, is discussed later.

Nonlinear regression of data for a system described by Scheme I using Eq. 25 with known values for  $k_{1p}$  and  $k_{p1}$  allows estimation of  $k'_{12}$  and  $k'_{21}$ . The ratio ( $k'_{12}/k'_{21}$ ) should estimate the partition coefficient,  $K_D$  (Eq. 23).

## EXPERIMENTAL

Ideal properties to test the theory were defined as follows. The solute should not contain any acidic or basic groups but should remain neutral throughout the pH range studied. (Alternatively, it should have a constant ionic form throughout the studies.) This condition eliminates the complication of a pH-dependent distribution coefficient. A simple stability-indicating assay is required. It must be possible to determine  $K_D$ ,  $k'_{12}$ , and  $k'_{21}$  under conditions where the solute is stable. The value for  $K_D$  must be sufficiently small to allow accuracy in the estimation of both  $k'_{12}$  and  $k'_{21}$ . Sink conditions ( $k'_{12} \gg k'_{21}$ ), which prevent the estimation of  $k'_{21}$ , eliminated the use of several nonaqueous solvents. The rate constants for degradation,  $k_{1p}$  and  $k_{p1}$ , must be on the same order of magnitude as  $k'_{12}$  and  $k'_{21}$  to prevent domination by either extraction or degradation. The solute should not undergo self-association so that  $K_D$  remains constant throughout the experiment.

UV absorption<sup>1</sup> was automatically recorded with a flowcell to monitor the  $C_1$  time course continuously. Absorbance at a single wavelength was related directly to  $C_1$  by selecting a solute whose degradation product did not interfere.

The  $\alpha, \beta$ -unsaturated ketone, cyclohept-2-enone (I), was chosen since it was expected to undergo hydrogen-ion-catalyzed hydration to the nonchromophoric compound, 3-hydroxycycloheptanone (II). Previous studies indicated that the process is reversible and that some reaction conditions do not favor complete hydration (20, 21).

In Scheme II, the concentration of I is given by:

$$C_1 = \frac{C_1^0 k_{1p}}{(k_{1p} + k_{p1})} e^{-(k_{1p} + k_{p1})t} + \frac{C_1^0 k_{p1}}{(k_{1p} + k_{p1})} \quad (\text{Eq. 26})$$

The negative slope,  $k_{app}$ , of a plot of  $\ln(C_1 - C_1^*)$  versus  $t$ , where  $C_1^* = C_1^0 k_{p1} / (k_{1p} + k_{p1})$ , is the sum of the first-order rate constants ( $k_{1p} + k_{p1}$ ). The reverse and forward constants may be calculated from:

$$k_{p1} = k_{app} C_1^* / C_1^0 \quad (\text{Eq. 27})$$

and:

$$k_{1p} = k_{app} - k_{p1} \quad (\text{Eq. 28})$$

The 233-nm absorption maximum of cyclohept-2-enone decreased to <5% of its initial value in 1 N HCl at 37° within 24 hr. A similar trial using cyclohex-2-enone produced a 32% reduction in 60 hr. The percent residual absorption of cyclohept-2-enone increased with decreasing acid strength.

The theory relating to Scheme I indicates that nonlinear regression based on Eq. 25 can be used to estimate  $k'_{12}$  and  $k'_{21}$  if the values for  $k_{1p}$  and  $k_{p1}$  (which may be assessed independently) are known. Equation 23 shows that the partition coefficient may be calculated from the ratio of the distribution constants,  $K_D = (k'_{12}/k'_{21})$ .

Estimates for  $K_D$  were similar at three initial concentrations, representing the range observed in the aqueous phase during partitioning kinetics. Determinations were made by equilibration of cyclohept-2-enone between equal volumes of water and light liquid petrolatum at 37° using the UV absorbance of the solute in the aqueous phase ( $\lambda_{max} = 233$  nm,

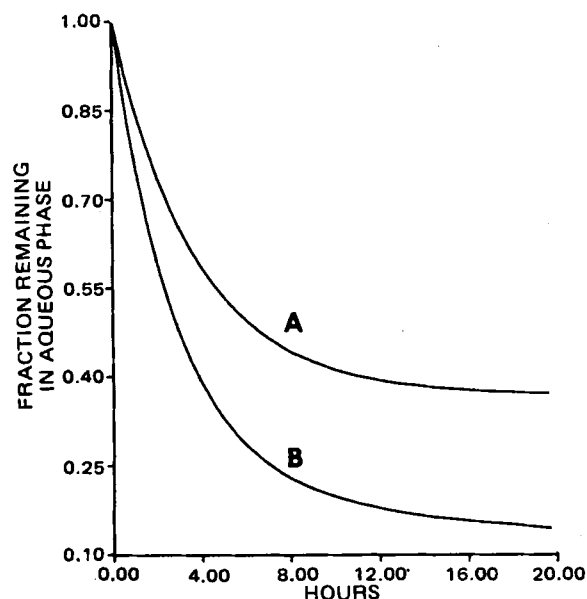


Figure 3—Fraction of the initial concentration of cyclohept-2-enone remaining in the raffinate as a function of time at 37° under stable (curve A) and unstable (curve B; 0.1 N HCl at 37°) conditions at 50 rpm in the transfer cell. The continuous data presented in the figure are indistinguishable from the theoretical curves obtained using Eq. 10 (curve A) and Eq. 25 (curve B) when  $k'_{12}$ ,  $k'_{21}$ ,  $k_{1p}$ , and  $k_{p1}$  values are as given in Table I.

$\epsilon = 10,182$ ). Control experiments to determine the partitioning of the solute between potassium chloride solutions of varying ionic strength ( $\mu = 0-1$ ) and light liquid petrolatum at 37° showed that  $K_D$  was independent of  $\mu$ . Prior to use, the light liquid petrolatum was extracted repeatedly with double-distilled water until the extracts showed no absorption at 233 nm and both phases were preequilibrated.

Distribution rate constants were estimated by introducing the solute into the aqueous phase of a transfer cell (Fig. 1) containing 90 ml of each preequilibrated phase, stirred<sup>2</sup> at 50 or 100 rpm and maintained at 37°. The initial concentration in the aqueous phase was  $1.4 \times 10^{-4}$  M. The aqueous phase was pumped<sup>3</sup> through a flowcell in the thermally controlled spectrophotometer. The 233-nm absorbance was recorded automatically as a function of time until equilibrium was attained. Final values agreed with the nonkinetic partitioning studies. Cyclohept-2-enone underwent <3% hydration after 96 hr under the study conditions. First-order plots based on Eq. 10 were linear for >95% of the process;  $k'_{12}$  and  $k'_{21}$  were calculated from Eqs. 23 and 24.

The kinetics of cyclohept-2-enone hydration were studied as a function of the hydrochloric acid concentration at 37°. Rate constants,  $k_{1p}$  and  $k_{p1}$ , were calculated from Eqs. 27 and 28; those in 0.1 N HCl were considered best for the evaluation of  $k'_{12}$  and  $k'_{21}$  under competing conditions. The residual absorbance after equilibration in 0.1 N HCl was 10.3% and is attributed to I since the contribution by II is negligible (20, 21).

The kinetics of hydration in 0.1 N HCl with simultaneous partitioning into light liquid petrolatum were measured in a stirred transfer cell at 50 or 100 rpm at 37°. Absorbance data (A at  $\lambda_{max} = 233$  nm) were analyzed by nonlinear regression (22) based on Eq. 25 where  $C_1 = A/\epsilon$ . Equilibration studies of I between 0.1 N HCl and light liquid petrolatum gave observed values for Z similar to those calculated from  $Z = C_1^0 k_{12} k_{p1} / \gamma \delta$  (Eq. 25). This agreement is consistent with the formation of a nonchromophoric product that does not partition significantly (Scheme I). The values for  $k'_{12}$  and  $k'_{21}$ , obtained in these experiments with simultaneous partitioning and hydration, were compared to those determined in the absence of hydration.

## RESULTS AND DISCUSSION

Curve A in Fig. 3 shows a typical time course for the fraction of solute remaining in the aqueous phase of a stirred transfer cell containing equal volumes of water and light liquid petrolatum at 37° and 50 rpm. The

<sup>1</sup> Models 250 and 6051, Gilford Instruments, Oberlin, Ohio.

<sup>2</sup> Model 53 dissolution stirrer, Hanson Research Corp., Northridge, Calif.

<sup>3</sup> Model 396/2396 minipump, Milton Roy Co., Riviera Beach, Fla.

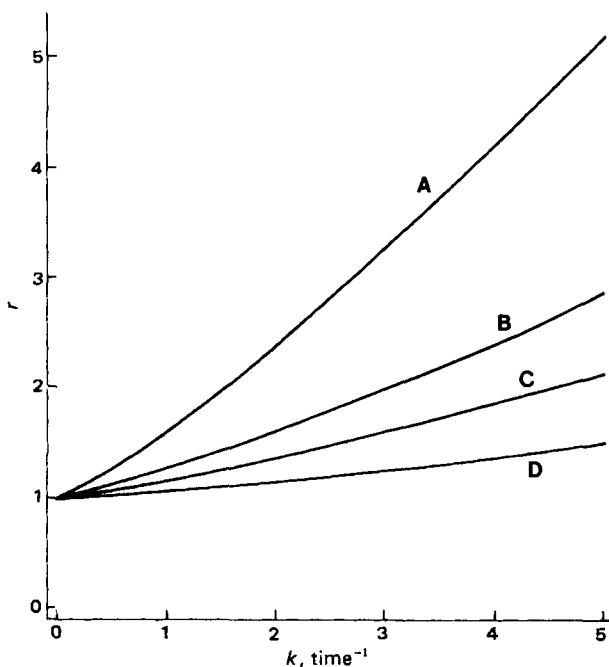
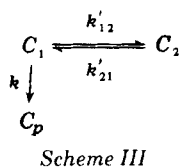


**Figure 4**—Relationship between  $r$  (calculated from Eq. 32) and  $K_D$  (Eq. 1) as a function of the relative values of  $k_{12}$ ,  $k_{21}$ , and  $k$ . In this illustration,  $k_{12} = k_{21}$ , so that  $K_D = 1$ , which is the value for  $r$  when  $k = 0$ . The  $k_{12}$  and  $k_{21}$  values are 1 (curve A), 2 (curve B), 3 (curve C), and 6 (curve D).



negative slope,  $S$ , of a first-order plot based on Eq. 10 was used to calculate  $k_{12}$  and  $k_{21}$  (Eqs. 23 and 24) from such data. Since cyclohept-2-enone is a neutral molecule, its  $K_D$  value should be independent of pH. Thus, the values determined for  $k_{12}$  and  $k_{21}$  under stable conditions should be the same as those determined in the presence of simultaneous degradation.

When the experiment was repeated with 0.1 N HCl as the aqueous phase, cyclohept-2-enone loss (Fig. 3, curve B) was described by Eq. 25 in accordance with Scheme I. Data were analyzed by nonlinear regression (22) of the entire time course to reiterate the values for  $k_{12}$  and  $k_{21}$  while assigning to  $k_{1p}$  and  $k_{p1}$  the values determined independently in 0.1 N HCl saturated with light liquid petrolatum at 37°. The agreement between the regression estimates and those determined independently (Table I) supports the proposed theory in which  $K_D = k_{12}/k_{21}$ .

The calculation of  $K_D$  under unstable conditions may be important to the chemist concerned with its modification. This approach can provide values that may be needed for structural correlations on partitioning. It may not be possible to determine  $K_D$  independently as was done with cyclohept-2-enone. For example, the solute may exist as a different charge species at pH values where it is stable, or conditions sufficiently stable for equilibration may not exist.

**Partitioning Kinetics with Simultaneous Irreversible Loss of Drug**—The present study demonstrated that biexponential loss from the aqueous phase of Scheme I can be analyzed for  $k_{12}$  and  $k_{21}$  whose ratio ( $k_{12}/k_{21}$ ) is  $K_D$ . This theory can be extended to Scheme III, which shows the irreversible loss of drug competing with the process of distribution as discussed previously (23) in reference to apomorphine distribution into the brains of mice. This process is analogous to the reversible first-order transfer of a compound between the aqueous phase,  $C_1$ , and the organic phase,  $C_2$ , of a stirred transfer cell with simultaneous, irreversible, first-order degradation to the product,  $C_p$ , in the aqueous phase. Applying the initial conditions of  $C_1 = C_1^0$  and  $C_2 = C_p = 0$  and again assuming that  $[A/V_1] = [A/V_2]$  remains constant provide:

$$C_1 = X'e^{-\alpha t} + Y'e^{-\beta t} \quad (\text{Eq. 29})$$

**Table I**—Comparison of the Rate Constants  $k'_{12}$  and  $k'_{21}$  for Distribution of Cyclohept-2-enone between Light Liquid Petrolatum and Water to the Estimates Obtained with Simultaneous Hydration and Partitioning (Light Liquid Petrolatum-0.1 N HCl) in a Stirred Transfer Cell at 37°

Revolutions per Minute	Stable Conditions			Simultaneous Loss <sup>a</sup>		
	$k'_{12}$	$k'_{21}$	$K_D^b$	$k'_{12}$	$k'_{21}$	Percent Error <sup>c</sup>
50	0.168	0.098	1.7	0.163	0.105	-5.9
100	0.206	0.120	1.7	0.210	0.130	-5.9

<sup>a</sup> The  $k'_{12}$  and  $k'_{21}$  values were determined by nonlinear regression based on Eq. 25;  $k_{1p}$  and  $k_{p1}$  were held constant at 0.117 and 0.0134 hr<sup>-1</sup>, respectively. <sup>b</sup>  $K_D = C_2^0/C_1^0 = k_{12}/k_{21}$ . <sup>c</sup>  $[(k_{12}/k_{21})^a - K_D]/K_D \times 100 = \text{percent error}$ .

where  $X' = C_1^0(\alpha - k'_{21})/(\alpha - \beta)$ ,  $Y' = C_1^0(k'_{21} - \beta)/(\alpha - \beta)$ ,  $\alpha = 0.5(K_3 + \sqrt{K_3^2 - 4k'_{21}k})$ ,  $\beta = 0.5(K_3 - \sqrt{K_3^2 - 4k'_{21}k})$ , and  $K_3 = (k'_{12} + k'_{21} + k)$ . The time course for solute concentration in the extract may be defined by:

$$C_2 = Z'(e^{-\beta t} - e^{-\alpha t}) \quad (\text{Eq. 30})$$

where  $Z' = C_1^0 k'_{12}/(\alpha - \beta)$ . Such a system, involving the simultaneous partitioning and hydrolysis of ampicillin and amoxicillin in isobutanol-aqueous hydrochloric acid, was investigated (24).

The observed phase ratio,  $C_2/C_1$ , will change as a function of time. The time required for this ratio to approach a constant value during an experiment depends on the values for  $k'_{12}$ ,  $k'_{21}$ , and  $k$ . When the contribution of the first term in Eq. 29 ( $X'e^{-\alpha t}$ ) becomes insignificant relative to the second term ( $Y'e^{-\beta t}$ ), the ratio approaches a constant. The time required for this result to occur,  $t_d$ , may be estimated from:

$$t_d \approx [\ln(F/R)]/(\beta - \alpha) \quad (\text{Eq. 31})$$

where  $R = (k'_{21} - \alpha)/(k'_{12} - \beta)$  and  $F$  is the fraction of  $C_1$  (Eq. 29) at  $t_d$  that is due to  $X'e^{-\alpha t}$  (25). If, for example, a contribution of 1% is considered insignificant, then  $F = 0.01$ . At  $t > t_d$ ,  $C_2/C_1$  (Scheme III) approaches a constant distribution ratio, which may be estimated from:

$$r = k'_{12}/(k'_{21} - \beta) \quad (\text{Eq. 32})$$

in the limit as  $X'e^{-\alpha t}$  approaches zero. Provided that  $t_d$  is not too large,  $C_2/C_1$  will approach  $r$  during the experiment. However, the value for  $r$  will not approximate  $K_D$  except under conditions in which the drug is relatively stable and  $(k'_{21} - \beta) \rightarrow k'_{21}$ .

The situation in which  $C_2/C_1$  may be described by  $r$  rather than by  $K_D$  is referred to as kinetic control of distribution in contrast to thermodynamic control (23). Although many successful biological correlations have been achieved using  $K_D$  values, there may be situations where kinetic control dominates. It was noted (23) that the distribution of norapomorphine to the brain [reported by Burkman *et al.* (26)] might be an example where competing kinetic processes controlled the brain-blood ratios,  $r$ , due to simultaneous drug loss by glucuronidation. It was suggested that  $t_d$  was too large to allow the observation of a constant  $r$  value before complete loss of the drug from the animal.

Another example where  $r$  may be of greater value than  $K_D$  is in simultaneous first-order absorption and degradation. This situation might occur through chemical degradation caused by stomach acidity or metabolism by intestinal flora. Tomlinson *et al.* (24) compared  $r$  and  $K_D$  values for amoxicillin and ampicillin under unstable conditions and discussed the potential significance of kinetic control of the phase ratios.

Figure 4 illustrates the relationship between  $r$  and  $K_D$  as a function of selected relative values for  $k_{12}$ ,  $k_{21}$ , and  $k$  (Scheme III). When  $k = 0$ ,  $r = K_D$ . From a practical viewpoint,  $r \approx K_D$  (within 5%) when  $(k_{12} + k_{21}) \geq 20k$ . As the  $k$  value increases,  $r$  increases relative to  $K_D$ , and kinetic control becomes increasingly significant.

**Conclusion**—A stirred transfer cell has been employed to calculate the partition coefficient,  $K_D$ , for a compound that is unstable in the aqueous phase. Equations for drugs that degrade irreversibly in one of the transfer cell phases (Scheme III) can simultaneously estimate the first-order rate constants for both degradation and distribution. This calculation, using kinetic methods, provides  $K_D$  values under conditions where equilibration experiments are not possible. These constants may be used to calculate  $K_D$ ,  $r$ , and the time at which distribution is considered complete ( $t > t_d$ ,  $F = 0.01$ ) as simultaneous irreversible degradation competes with partitioning. The difference between  $r$  and  $K_D$  indicates the degree of kinetic control for the system.

## REFERENCES

- (1) W. G. Whitman, *Chem. Metall. Eng.*, **29**, 146 (1923)
- (2) W. K. Lewis and W. G. Whitman, *Ind. Eng. Chem.*, **16**, 1215 (1924).
- (3) K. F. Gordon and T. K. Sherwood, *Chem. Eng. Progr. (Symp. Ser.)*, **50**, 15 (1954).
- (4) T. K. Sherwood and K. F. Gordon, *AIChE J.*, **1**, 129 (1955).
- (5) R. E. Treybal, "Liquid Extraction," 2nd ed., McGraw-Hill, New York, N.Y., 1963, pp. 173-182.
- (6) J. T. Davies and E. K. Rideal, "Interfacial Phenomena," Academic, New York, N.Y., 1961, pp. 311-321.
- (7) T. K. Sherwood, R. L. Pigford, and C. R. Wilke, "Mass Transfer," McGraw-Hill, New York, N.Y., 1975, pp. 178-181.
- (8) W. J. McManamey, J. T. Davies, J. M. Woollen, and J. R. Coe, *Chem. Eng. Sci.*, **28**, 1061 (1973).
- (9) H. P. Ting, G. L. Bertrand, and D. F. Sears, *Biophys. J.*, **6**, 813 (1966).
- (10) T. Higuchi and A. F. Michaelis, *Anal. Chem.*, **40**, 1925 (1968).
- (11) P. B. McNulty, *J. Pharm. Sci.*, **64**, 1500 (1975).
- (12) H. L. Rosano, P. Duby, and J. H. Schulman, *J. Phys. Chem.*, **65**, 1704 (1961), and references cited therein.
- (13) B. C. Lippold and G. F. Schneider, *Arzneim.-Forsch.*, **25**, 843 (1975).
- (14) *Ibid.*, **25**, 1683 (1975).
- (15) *Ibid.*, **26**, 2202 (1976).
- (16) B. C. Lippold and G. F. Schneider, *Pharmazie*, **31**, 237 (1976).
- (17) H. Kubinyi, *J. Pharm. Sci.*, **67**, 262 (1978).
- (18) G. L. Flynn, S. H. Yalkowsky, and T. J. Roseman, *ibid.*, **63**, 479 (1974).
- (19) L. Benet, *ibid.*, **61**, 536 (1972).
- (20) R. E. Notari and S. M. Caiola, *ibid.*, **58**, 1203 (1969).
- (21) E. R. Garrett and R. E. Notari, *J. Org. Chem.*, **31**, 425 (1966).
- (22) C. M. Metzler, G. L. Elfring, and A. J. McEwen, *Biometrics*, **30** (3) (1974).
- (23) R. E. Notari, *Pharm. Weekbl.*, **110**, 577 (1975).
- (24) E. Tomlinson, R. E. Notari, and P. R. Byron, *J. Pharm. Sci.*, in press.
- (25) P. R. Byron and R. E. Notari, *ibid.*, **65**, 1140 (1976).
- (26) A. M. Burkman, R. E. Notari, and W. K. Van Tyle, *J. Pharm. Pharmacol.*, **26**, 493 (1974).

## 2-<sup>14</sup>C-1-(2'-Deoxy-β-D-ribofuranosyl)-5-ethyluracil: Synthesis and Biotransformation in Rats

RAVINDER KAUL\*, GEBHARD KIEFER, SIEGFRIED ERHARDT, and BERND HEMPEL

Received December 15, 1975, from the Research Laboratories, Pharmaceuticals Robugen GmbH, Alleenstrasse 22, D-73 Esslingen-Zell, West Germany. Accepted for publication November 29, 1978.

**Abstract** □ With <sup>14</sup>C-urea as the starting material, 2-<sup>14</sup>C-1-(2'-deoxy-β-D-ribofuranosyl)-5-ethyluracil [2-<sup>14</sup>C-β-5-ethyl-2'-deoxyuridine] was synthesized for metabolic studies. After intravenous administration in rats, the radioactivity disappeared in the blood within 72 hr, being eliminated primarily in the urine (97%). The major elimination took place in the first 24 hr (92%). Little radioactivity was detected in the organs and tissues after 3 days. Approximately 50% of the urine radioactivity probably was due to an unidentified conjugate, 30% was due to Metabolite II, and 20% was unchanged drug. Metabolite II was identified as 5-ethyluracil by mass and <sup>1</sup>H-NMR spectra and by comparison with an authentic sample.

**Keyphrases** □ Ethyldeoxyuridine—synthesis, biotransformation in rats, metabolites □ Antiviral agents—ethyldeoxyuridine, synthesis, biotransformation in rats, metabolites

1-(2'-Deoxy-β-D-ribofuranosyl)-5-ethyluracil (β-5-ethyl-2'-deoxyuridine<sup>1</sup>, VIII) has shown promising therapeutic activity against herpes simplex and vaccina viruses (1, 2) and against herpes keratitis in rabbits (3). Due to its compatibility with the ophthalmic mucous membrane, VIII is particularly suitable for the treatment of herpetic eye disease (4-7). Its excretion, distribution, and biotransformation were studied in rats using <sup>14</sup>C-VIII.

### EXPERIMENTAL<sup>2</sup>

**Synthesis**—For metabolic studies, <sup>14</sup>C-β-5-ethyl-2'-deoxyuridine (VIII), specific activity 0.168 mCi/mole, was synthesized (Scheme I). The starting material was <sup>14</sup>C-urea<sup>3</sup>, specific activity 5.13 mCi/mole.

<sup>1</sup> Edurid, Robugen GmbH, 7300 Esslingen/Neckar, West Germany.

<sup>2</sup> Melting points were taken on a Tottoli (Büchi, Switzerland) apparatus and are uncorrected. Mass spectra were measured at an ionizing potential of 70 eV with a CH-7 Varian MAT spectrometer using a direct evaporator inlet system. <sup>1</sup>H-NMR spectra were recorded on a Varian T-60 spectrometer using dimethyl sulfoxide-*d*<sub>6</sub> as the solvent and trimethylsilane as the internal standard.

<sup>3</sup> New England Nuclear Corp., Boston, Mass.

2-<sup>14</sup>C-5-Ethylbarbituric Acid (III)—Diethyl ethylmalonate (II) (9.4 g, 0.05 mole) was added dropwise to 10 ml of a 30% methanolic sodium methoxide solution. The reaction mixture was refluxed for 30 min with constant stirring. Then the <sup>14</sup>C-urea solution (3 g, 0.05 mole) in 10 ml of methanol was added quickly. The reaction mixture was refluxed with stirring for 6 hr under anhydrous conditions.

After cooling, the solvent was evaporated to dryness, and the residue was dissolved in 30 ml of hot water. The solution was acidified to pH 1-2 with 10 ml of concentrated hydrochloric acid. Crystals that precipitated overnight under refrigeration were filtered off, washed with ice water, and dried to yield 6.1 g of 2-<sup>14</sup>C-III (78.3% based on <sup>14</sup>C-urea), mp 195-197° [lit. (8) mp 194-195°, (9) mp 193-194°].

2-<sup>14</sup>C-5-Ethyl-6-chlorouracil (IV)—Phosphoryl chloride (14 ml) was added dropwise into a mixture of III (6.1 g, 0.035 mole) and water (0.5 ml). The reaction mixture temperature was slowly raised to 100° with constant stirring. After heating on an oil bath for 90 min at 90-100°, the reaction mixture was cooled. The remaining phosphoryl chloride was decomposed carefully with 25 ml of water.

The cooled mixture was stirred for 1 hr and allowed to stand in the refrigerator overnight. The white crystalline precipitate was filtered off, washed with ice water, and dried to yield 6.1 g of 2-<sup>14</sup>C-IV (70% based on <sup>14</sup>C-urea), mp 215-217° [lit. (10) mp 215-217°].

2-<sup>14</sup>C-5-Ethyluracil (V)—The solution of IV (6.1 g, 0.035 mole) in 2 N NaOH (58 ml) and 1% palladium-on-charcoal was hydrogenated at 60°. The hydrogen uptake virtually ceased after 3 hr. The catalyst was filtered off, and the filtrate was acidified with concentrated hydrochloric acid. After cooling, the precipitated crystals were filtered off, washed with cold water, and dried to yield 3.6 g of 2-<sup>14</sup>C-V (51.4% based on <sup>14</sup>C-urea), mp 308-309° [lit. (8) mp 302-303°, (11, 12) mp 300-303°, (13) mp 300°, (14, 15) mp 308-309°].

2-<sup>14</sup>C-2,4-Bis-O-(trimethylsilyl)-5-ethylpyrimidine (VI)—Compound V (3.6 g, 25.5 mmoles), hexamethyldisilazane (21 ml), and dimethylformamide (1.8 ml) were heated on an oil bath for 12 hr at 160-170° with constant stirring under anhydrous conditions. After cooling, the solvent was removed under reduced pressure. The residue, an oily yellow liquid, was used without further purification in the next step.

2-<sup>14</sup>C-1-(3',5'-Di-O-p-chlorobenzoyl-2'-deoxy-α,β-D-ribofuranosyl)-5-ethyluracil (VIIa and VIIb)—The reaction of VI with 3,5-di-O-p-chlorobenzoyl-2'-deoxy-α,β-D-ribofuranosyl chloride (16) to produce 1-(3',5'-di-O-p-chlorobenzoyl-2'-deoxy-α,β-D-ribofuranosyl)-5-substi-